USArray shear wave splitting shows seismic anisotropy from both lithosphere and asthenosphere

Sutatcha Hongsresawat[1], Mark P. Panning[1], Raymond M. Russo[1], David A. Foster[1], Vadim Monteiller[2]*, and Sébastien Chevrot[2]

[1]Department of Geological Sciences, University of Florida, PO Box 112120, Gainesville, Florida 32611-2120, USA

[2]Institut de Recherche en Astrophysique et Planétologie, Observatoire Midi Pyrénées, CNRS, UMR 5277, Université Paul Sabatier, Toulouse, 14 Avenue Edouard Belin, F-31400 Toulouse, France

ABSTRACT

North America provides an important test for assessing the coupling of large continents with heterogeneous Archean- to Cenozoic-aged lithospheric provinces to the mantle flow. We use the unprecedented spatial coverage of the USArray seismic network to obtain an extensive and consistent data set of shear wave splitting intensity measurements at 1436 stations. Overall, the measurements are consistent with simple shear deformation in the asthenosphere due to viscous coupling to the overriding lithosphere. The fast directions agree with the absolute plate motion direction with a mean difference of 2° with 27° standard deviation. There are, however, deviations from this simple pattern, including a band along the Rocky Mountain front, indicative of flow complication due to gradients in lithospheric thickness, and variations in amplitude through the central United States, which can be explained through varying contributions of lithospheric anisotropy. Thus, seismic anisotropy may be sourced in both the asthenosphere and lithosphere, and variations in splitting intensity are due to lithospheric anisotropy developed during deformation over long time scales.

INTRODUCTION

North America is a rich target for geophysical studies due to its diverse tectonics, ranging from Cenozoic to recent active tectonics in the west, to stable continental craton in the center, to Mesozoic oceanic lithosphere in the east. Shear wave splitting observations are a powerful tool to investigate the geometry of deformation in the upper mantle. SKS waves are commonly used to image anisotropic fabrics beneath seismic stations (Vinnik et al., 1984; Silver and Chan, 1991) resulting from alignment of minerals in the lithosphere or underlying asthenosphere. Shear in the asthenosphere due to viscous coupling at the base of lithospheric plates or vertical coherent deformation through the crust and lithosphere during tectonic interactions are both invoked as mechanisms for fabric development. Interpretations of the splitting data are limited by seismic station locations, so continental-scale interpretations require an extensive seismic array. The deployment of the USArray Transportable Array (TA) seismic network, which covers much of the United States with ~70 km station spacing, permits imaging of mantle fabric beneath North America. The two-year recording period for each station yields a sufficient number of seismograms from earthquakes in the optimal magnitude and distance range to obtain good splitting.

Upon entering an anisotropic volume, a shear wave splits into a fast wave polarized parallel to the fabric symmetry axis and an orthogonally polarized slow wave. These waves arrive at a station with a time separation due to their velocity difference. We determine a delay time, δt, and fast polarization azimuth, φ, of the layer from the seismic waveforms. These observations are interpreted to reflect either current asthenospheric plastic flow or fabrics due to older tectonic deformations (Silver, 1996).

METHODS

Instead of using standard procedures such as the Silver and Chan method (Silver and Chan, 1991) for determining SKS splitting parameters, φ and δt, from individual seismograms, we employ a multichannel method (Chevrot, 2000) by fitting a sinusoid to a new quantity, splitting intensity, *SI*, as a function of back-azimuth of sources. The advantage of this method is the use of records from many back-azimuths even if the signal to noise ratio is low. The amplitude and phase of the fit to the back-azimuthal dependence yield δt and φ, respectively. φ is interpreted as the preferred orientation of the fast axes (*a*) of olivine crystals, and δt is related to the strength and/or thickness of the anisotropic layer. Modeling observations at a station with a single φ and δt is equivalent to assuming a single anisotropic layer, which is not required for modeling splitting intensity (e.g., Monteiller and Chevrot, 2011), but useful for visualization of a large data set and comparison with other splitting measurements.

The measurements are made on 860,000 seismic traces recorded at 1436 USArray TA stations. For each station, we record ~200 magnitude 6–7 teleseismic earthquakes with good back-azimuthal coverage (see Fig. DR1 in the GSA Data Repository[1]). In the epicentral distance range used, 87°–120°, the SKS phase is well resolved without interference of other high-amplitude phases such as S and ScS. All seismograms are processed in the same way: (1) the SKS phase arrival was determined visually; (2) SKS horizontal components were rotated to radial and transverse components; and (3) a low-pass fourth-order Butterworth filter with minimum period of 10 s was applied. We then compute splitting intensity using MATLAB interfaces (Monteiller and Chevrot, 2011). For δt values that are small (<2.5 s) in comparison with the dominant period of the SKS wave (>10 s), *SI* is measured by projecting the transverse component, $T(t)$, on the radial component derivative, $R'(t)$:

$$\mathrm{SI} = -2\frac{\int T(t)R'(t)\,dt}{\int R'^2(t)}. \quad (1)$$

SPLITTING INTENSITY MEASUREMENTS

We present splitting measurements (Fig. 1) at USArray TA and Caltech (California Institute of Technology) Regional Seismic Network (CI) stations (Monteiller and Chevrot, 2011). These splitting parameters are typically derived from ≥30 high-quality splitting intensity measurements at each station. The measurements show smooth variations of both splitting parameters over short distances, in contrast with results of several previous studies (Liu, 2009; Refayee et al., 2014). We also show directions of absolute plate motion (APM) of North America computed from the model HS3-NUVEL 1A (Gripp and Gordon, 2002), with a fixed hotspot frame of reference (other reference frames are shown in Figure DR2).

We observe a complex pattern of splitting in the western part of North America (Fig. 1). φ trends in Southern California deviate from a general

*Current address: Géoazur, Université de Nice Sophia-Antipolis, CNRS, Observatoire de la Côte d'Azur, 250 Rue Albert Einstein, Sophia Antipolis, 06560 Valbonne, France.

[1]GSA Data Repository item 2015234, comparisons between our measurements and 7 additional plate velocity models, is available online at www.geosociety.org/pubs/ft2015.htm, or on request from editing@geosociety.org or Documents Secretary, GSA, P.O. Box 9140, Boulder, CO 80301, USA.

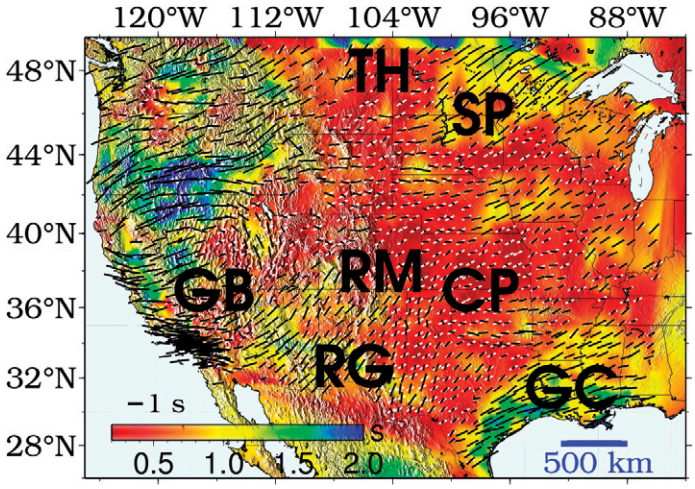

Figure 1. SKS splitting measurements at USArray Transportable Array stations plotted on topography of North America. Black lines are orientation of fast polarization directions, φ, line length is proportional to delay time, δ*t*, and colors represent interpolated δ*t* among stations. White lines are absolute plate motion directions based on fixed hotspot model HS3-NUVEL 1A (Gripp and Gordon, 2002). CP—Central Plain; GB—Great Basin; GC—Gulf Coast; RG—Rio Grande Rift; RM—Rocky Mountains; SP—Superior province; TH—Trans-Hudson orogen. A line length representing 1 s delay time is shown in the lower left.

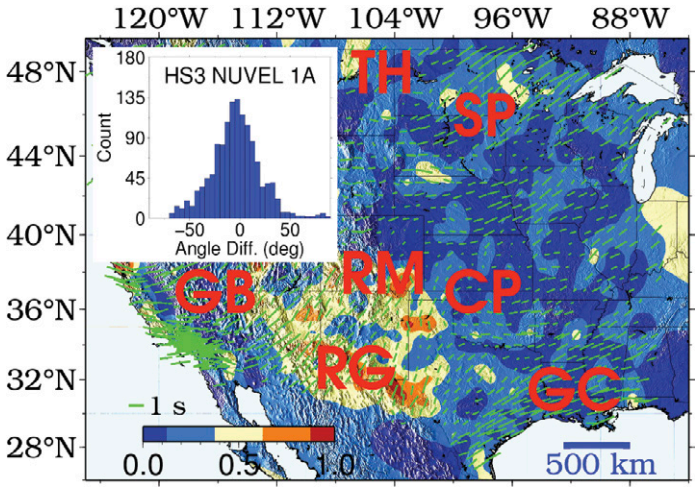

Figure 2. Splitting results plotted on scaled difference between measured fast polarization azimuth (φ) values and absolute plate motion (APM) direction at station locations. Colors represent calculated difference *D* (in seconds; see text for definition). Labels of geological regions are same as in Figure 1. Inset shows histogram of angular difference (Diff.) between φ and APM directions calculated from the fixed hot-spot plate motion model HS3 NUVEL 1A, which is widely accepted to represent the motion of the overlying lithosphere. A line length representing 1 s delay time is shown in the lower left.

northeast-southwest trend of most of our measurements. In the Great Basin, we observe a pattern of fast polarization alignment in semicircles, confirming similar observations by Savage and Sheehan (2000), Liu (2009), and West et al. (2009). In the Central Plains and within the Trans-Hudson orogen, δ*t* values are consistently less than 0.5 s, in contrast with the 1 s reported earlier (Silver, 1996; Fouch et al., 2000; Schutt and Humphreys, 2001; Refayee et al., 2014). Our measurements reveal an increase in δ*t* values from ~0.5 to >1 s in both the Gulf Coast and Superior province. Both regions with amplified δ*t* are distinct and defined by measurements at >50 stations.

COMPARISON WITH APM

Anisotropy can reside in both the lithosphere and the asthenosphere. In the more rigid lithosphere, splitting measurements likely capture mantle fabrics produced by deformation during the tectonic evolution of North America (Silver, 1996). In contrast, current shear at the base of the lithosphere is the best candidate mechanism for aligning minerals in the asthenosphere (Vinnik et al., 1989). This sets up two simple end-member models: lithospheric fabrics should primarily parallel observed local geologic fabrics, but asthenospheric fabrics should align parallel to North America's current APM, although deviations may result from more complicated flow of the mantle (e.g., Becker et al., 2014).

In Figure 2, we plot our measurements on the scaled difference,

$$D = \delta t \sqrt{\left(\sin\varphi - \sin\varphi_{APM}\right)^2 + \left(\cos\varphi = \cos\varphi_{APM}\right)^2},$$

between φ and North America APM directions (φ_{APM}) computed from the fixed-hotspot model HS3-NUVEL 1A (Gripp and Gordon, 2002). The inset shows a histogram of angle differences between observed φ and local APM (mean difference 2°, 27° standard deviation) showing good agreement. Measured φ values are essentially parallel to APM at most stations, except in the region from the central Great Basin to the Rio Grande Rift and southern Rocky Mountains. Reds and oranges in this figure delimit the areas where we observe large disagreement between φ and φ_{APM}. A prominent deviation aligns with the Rocky Mountain front and the underlying boundary between thick cratonic lithosphere east of the front and thinner lithosphere to the west, suggestive of deviation of asthenospheric flow (e.g., Refayee et al., 2014). The clear agreement between observed φ and φ_{APM} supports the hypothesis that the source of most anisotropy is simple shear in the asthenosphere (Vinnik et al., 1989), but the regions of φ-φ_{APM} deviation reflect either significant contributions to splitting intensity from the North American lithosphere (Silver and Chan, 1991) or deviations of asthenospheric deformation from the simple shear model (Conrad and Behn, 2010). We note that the overall agreement with North American measurements with model HS3-NUVEL 1A (similar to the observation of Yuan et al. [2011]) is not present with all APM reference models (Fig. DR2). Other models generally include less net rotation of the lithosphere, suggesting that these SKS measurements can improve our understanding of coupling versus decoupling processes between the lithosphere and the mesosphere beneath North America once they are included in mantle dynamics and plate motion studies (e.g., Becker, 2008; Kreemer, 2009; Zheng et al., 2014). For comparison, we also compare to anisotropy predicted from a flow model with a good agreement to global anisotropy measurements (Fig. DR3; Becker et al., 2014), but the agreement is poor (mean difference of 33° at a depth of 200 km), likely due to the difficulty in modeling the influence of variable continental lithospheric keel (Becker, 2008).

COMPARISON WITH GEOLOGICAL BASEMENTS, MAGNETIC AND GRAVITY ANOMALIES, AND LITHOSPHERIC THICKNESS

To assess whether lithospheric anisotropy correlates with structural grain in crustal geological provinces, we plot our results over basement province boundaries, magnetic and gravity anomalies, and modeled lithospheric thickness (Fig. 3). Delay times within the Archean Superior province and along the Phanerozoic Gulf Coast are distinctly higher (>1 s) than those in the Proterozoic Central Plains (<0.5 s) (Fig. 3A). When compared with magnetic anomalies (Fig. 3B), a common proxy for basement geology texture (Maus, 2010), there is a strong correlation between the trends of magnetic anomalies and φ in the Superior province region. The effect of North America's lithospheric thickness is shown by comparing splitting with Bouguer gravity anomalies (Kucks, 1999) (Fig. 3C) and model lithospheric thickness (Yuan and Romanowicz, 2010; Yuan et al., 2011) (Fig.

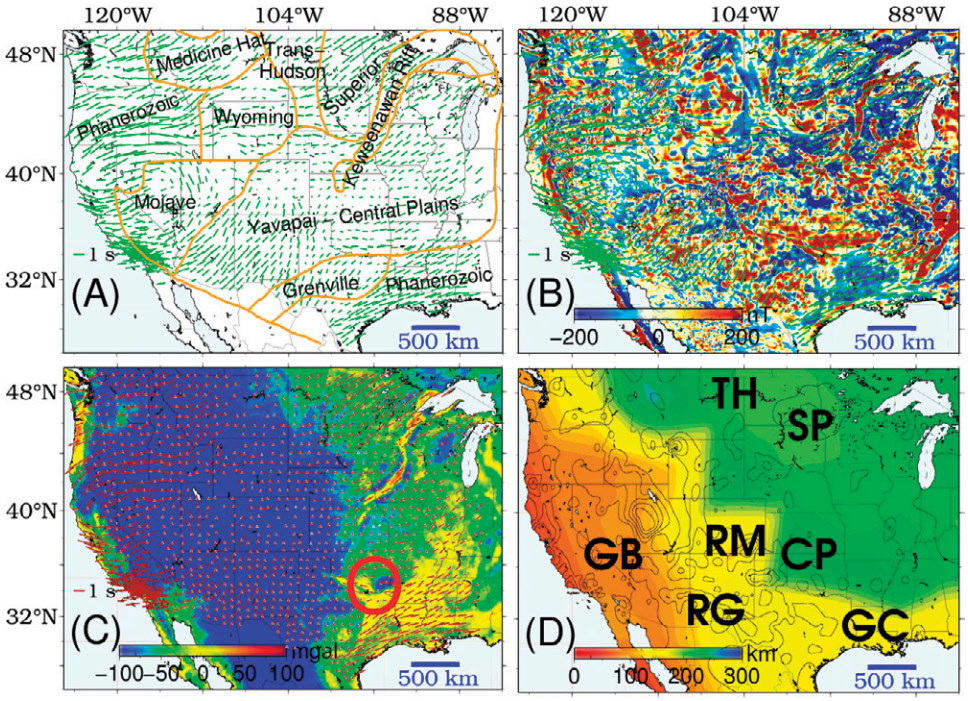

Figure 3. A: Splitting results plotted on geological basements of North America (Foster et al., 2006). A line length representing 1 s delay time is shown in the lower left of A–C. B: Splitting results plotted on magnetic anomalies (Maus, 2010). Color represents interpolated anomaly in nT. C: Splitting results plotted on Bouguer gravity anomalies (Kucks, 1999), with red circle showing location of Oklahoma aulacogen. Color represents interpolated anomalies in mgal. D: Contour map of scaled difference in Figure 2 in comparison with lithospheric thickness of North America (Yuan et al., 2011). Labels of geological regions are same as in Figure 1.

3D). The transition between thick and thin lithosphere is visible in the δt >1 s signal at Gulf Coast stations. Correlations between these δt values, low gravity anomalies, and thin lithosphere, and the agreement of fast directions and APM (Fig. 2), suggest an asthenospheric origin for anisotropy in the Phanerozoic Gulf Coast region. We note a strong signal with fast axes parallel to the trend of the Oklahoma aulacogen (red circle in Fig. 3C), a failed rift from the Neoproterozoic-Cambrian breakup of Rodinia (Gilbert, 1983).

Bokelmann and Wüstefeld (2009) proposed that magnetic anomalies in the crust and seismic anisotropy in the mantle are subparallel in the Superior province, and showed a correlation between alignments of magnetic anomalies and anisotropy for a few stations. We investigate this hypothesis by forward-modeling splitting intensity versus back-azimuth patterns (Chevrot, 2006) at two representative locations in the Trans-Hudson orogen (station C24A) and the Superior province (station B33A) (Fig. 4). Although φ trends in both regions are subparallel to local APM, we observe a contrast between δt estimates: $\delta t < 0.5$ s in the Tran-Hudson orogen, but $\delta t > 1.0$ s in the Superior province. We compare our measurements with magnetic anomalies (Fig. 4B), a proxy for lithospheric fabric, and highlight the average lithospheric fabric in the Trans-Hudson orogen (~0°) and Superior province (~70°). We define a two-layer anisotropic structure to model (Fig. 4C) The orientation of asthenospheric fabric beneath these two regions is set to the APM value of 67.5°, but the lithospheric fabrics between 30 and 200 km depth (chosen to match the lithospheric thickness determined by Yuan et al. [2011]) (Fig. 3D), are set according to magnetic fabrics. The anisotropy strength, γ, defined as the ratio of the square of the fast and slow shear velocities minus 1, is set to a uniform value of 0.02. We also assume that the incoming SKS waves arrive vertically, justifiable given actual incidence angles of 10°–13°. There is excellent agreement between our modeled and measured splitting intensities at both stations. Although the model chosen is non-unique, and there are tradeoffs between strength and thickness of anisotropic layers, this simple model explains contrasting measurements in areas with similar lithospheric thickness well. In the Superior province, which has a thick lithosphere and magnetic textures aligned with local APM, the observed $\delta t > 1$ s can be explained by the constructive delay time addition from both asthenospheric APM fabrics and lithospheric textures. In contrast, the smaller $\delta t < 0.5$ s of the Trans-Hudson orogen, which has equally thick

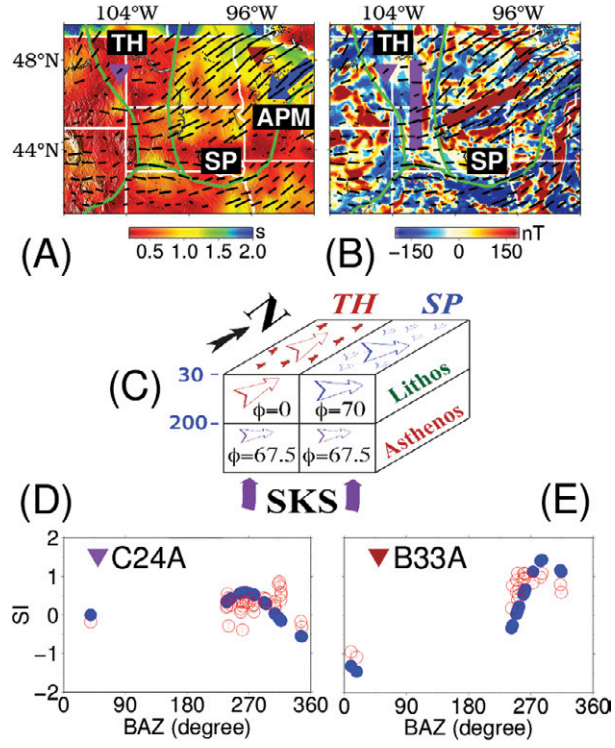

Figure 4. A: Splitting measurements in Trans-Hudson orogen (TH) and Superior province (SP) regions. Test stations C24A (purple inverted triangle) and B33A (brown inverted triangle) are shown. Black lines are orientation of fast polarization directions, green lines are geological basement boundaries, white lines are state boundaries, and scale bar shows range of delay time. Blue arrow is average absolute plate motion (APM) direction. B: Measurements plotted on top of magnetic anomaly map, which serves as proxy for lithospheric fabric. Purple and brown bars represent average angles of lithospheric fabric in these regions. C: Two-layer model diagram showing fast directions in all layers (Lithos—lithosphere; Asthenos—asthenosphere). D,E: Calculated back-azimuthal (BAZ) variations of splitting intensity at stations C24A and B33A. SI—splitting intensity. Open and filled circles are measured SI and calculated SI at these two stations, respectively.

lithosphere but magnetic trends that are ~70° from APM, can be explained by misalignment of lithospheric and asthenospheric fabrics. For the northern Great Lakes region, these variations of fabrics agree well with those reported at depths of 70 and 250 km by an independent three-dimensional full-waveform inversion study (Yuan et al., 2011). The conclusion of the importance of anisotropy in both the lithosphere and asthenosphere is consistent with previous studies including both surface waves and splitting measurements (e.g., Marone and Romanowicz, 2007; Yuan and Romanowicz, 2010; Yuan et al., 2011) as well as some local splitting studies (e.g., Levin et al., 1999; Deschamps et al., 2008). These results from splitting intensity across North America demonstrate the power of such measurements which allow for greater lateral resolution, comparable to station spacing, when compared to surface wave studies, while remaining sensitive to depth variations in anisotropic fabrics in a way that traditional SKS splitting measurements are not (e.g., Vinnik et al., 1989; Silver, 1996).

SUMMARY

The majority of our φ measurements parallel local APM trends, indicating that asthenospheric fabrics produced by shear between North American lithosphere and deeper mantle are the dominant source of observed shear wave splitting at TA stations. Deviations from this association from the Rocky Mountain front and to the east occur in two distinct regions: areas where lithospheric thickness varies on a short spatial scale, and regions where continental geologic fabrics, as defined by magnetic and gravity anomalies, do not parallel local APM trends. Splitting delay times are enhanced in regions where asthenospheric and lithospheric fabrics are subparallel. Specifically: (1) upper mantle fabrics beneath the southern Rocky Mountain region are complicated by the transition from thin to thick lithosphere, which causes deviations from APM directions (Fig. 3); (2) delay times attain a regional high value along the Gulf Coast due to strong asthenospheric APM fabrics in a region of thin lithosphere (Fig. 3); and (3) in the north-central United States, there is a contrast in observed splitting between the Superior province and the Trans-Hudson orogen where lithospheric texture alignment, relative to local APM, plays an important role in enhancing or diminishing delay times.

ACKNOWLEDGMENTS

We are grateful to Richard Gordon and Barbara Romanowicz, an anonymous reviewer, and editor Brendan Murphy for helpful comments. We thank Thorsten Becker for providing a model for comparison. This work was supported by grant EAR-1154039 from the National Science Foundation.

REFERENCES CITED

Becker, T.W., 2008, Azimuthal seismic anisotropy constrains net rotation of the lithosphere: Geophysical Research Letters, v. 35, L05303, doi:10.1029/2007GL032928.

Becker, T.W., Conrad, C.P., Schaeffer, A.J., and Lebedev, S., 2014, Origin of azimuthal seismic anisotropy in oceanic plates and mantle: Earth and Planetary Science Letters, v. 401, p. 236–250, doi:10.1016/j.epsl.2014.06.014.

Bokelmann, G.H., and Wüstefeld, A., 2009, Comparing crustal and mantle fabric from the North American craton using magnetics and seismic anisotropy: Earth and Planetary Science Letters, v. 277, p. 355–364, doi:10.1016/j.epsl.2008.10.032.

Chevrot, S., 2000, Multichannel analysis of shear wave splitting: Journal of Geophysical Research, v. 105, p. 21,579–21,590, doi:10.1029/2000JB900199.

Chevrot, S., 2006, Finite-frequency vectorial tomography: A new method for high-resolution imaging of upper mantle anisotropy: Geophysical Journal International, v. 165, p. 641–657, doi:10.1111/j.1365-246X.2006.02982.x.

Conrad, C.P., and Behn, M.D., 2010, Constraints on lithosphere net rotation and asthenospheric viscosity from global mantle flow models and seismic anisotropy: Geochemistry Geophysics Geosystems, v. 11, Q05W05, doi:10.1029/2009GC002970.

Deschamps, F., Lebedev, S., Meier, T., and Trampert, J., 2008, Stratified seismic anisotropy reveals past and present deformation beneath the East-central United States: Earth and Planetary Science Letters, v. 274, p. 489–498, doi:10.1016/j.epsl.2008.07.058.

Foster, D.A., Mueller, P.A., Mogk, D.W., Wooden, J.L., and Vogl, J.J., 2006, Proterozoic evolution of the western margin of the Wyoming craton: Implications for the tectonic and magmatic evolution of the northern Rocky Mountains: Canadian Journal of Earth Sciences, v. 43, p. 1601–1619, doi:10.1139/e06-052.

Fouch, M.J., Fischer, K.M., Parmentier, E., Wysession, M.E., and Clarke, T.J., 2000, Shear wave splitting, continental keels, and patterns of mantle flow: Journal of Geophysical Research, v. 105, p. 6255–6275, doi:10.1029/1999JB900372.

Gilbert, M.C., 1983, Timing and chemistry of igneous events associated with the Southern Oklahoma Aulacogen: Tectonophysics, v. 94, p. 439–455, doi:10.1016/0040-1951(83)90028-8.

Gripp, A.E., and Gordon, R.G., 2002, Young tracks of hotspots and current plate velocities: Geophysical Journal International, v. 150, p. 321–361, doi:10.1046/j.1365-246X.2002.01627.x.

Kreemer, C., 2009, Absolute plate motions constrained by shear wave splitting orientations with implications for hot spot motions and mantle flow: Journal of Geophysical Research, v. 114, B10405, doi:10.1029/2009JB006416.

Kucks, R.P., 1999, Bouguer gravity anomaly data grid for the conterminous US: U.S. Geological Survey, http://mrdata.usgs.gov/metadata/usgravboug.html (accessed 6 May 2015).

Levin, V., Menke, W., and Park, J., 1999, Shear wave splitting in the Appalachians and the Urals: A case for multilayered anisotropy: Journal of Geophysical Research, v. 104, p. 17,975–17,993, doi:10.1029/1999JB900168.

Liu, K.H., 2009, NA-SWS-1.1: A uniform database of teleseismic shear wave splitting measurements for North America: Geochemistry Geophysics Geosystems, v. 10, Q05011, doi:10.1029/2009GC002440.

Marone, F., and Romanowicz, B.A., 2007, The depth distribution of azimuthal anisotropy in the continental upper mantle: Nature, v. 447, p. 198–201, doi:10.1038/nature05742.

Maus, S., 2010, An ellipsoidal harmonic representation of Earth's lithospheric magnetic field to degree and order 720: Geochemistry Geophysics Geosystems, v. 11, Q06015, doi:10.1029/2010GC003026.

Monteiller, V., and Chevrot, S., 2011, High-resolution imaging of the deep anisotropic structure of the San Andreas Fault system beneath southern California: Geophysical Journal International, v. 186, p. 418–446, doi:10.1111/j.1365-246X.2011.05082.x.

Refayee, H.A., Yang, B.B., Liu, K.H., and Gao, S.S., 2014, Mantle flow and lithosphere-asthenosphere coupling beneath the southwestern edge of the North American craton: Constraints from shear-wave splitting measurements: Earth and Planetary Science Letters, v. 402, p. 209–220, doi:10.1016/j.epsl.2013.01.031.

Savage, M.K., and Sheehan, A.F., 2000, Seismic anisotropy and mantle flow from the Great Basin to the Great Plains, western United States: Journal of Geophysical Research, v. 105, p. 13,715–13,734, doi:10.1029/2000JB900021.

Schutt, D.L., and Humphreys, E.D., 2001, Evidence for a deep asthenosphere beneath North America from western United States SKS splits: Geology, v. 29, p. 291–294, doi:10.1130/0091-7613(2001)029<0291:EFADAB>2.0.CO;2.

Silver, P.G., 1996, Seismic anisotropy beneath the continents: Probing the depths of geology: Annual Review of Earth and Planetary Sciences, v. 24, p. 385–432, doi:10.1146/annurev.earth.24.1.385.

Silver, P.G., and Chan, W.W., 1991, Shear wave splitting and subcontinental mantle deformation: Journal of Geophysical Research, v. 96, p. 16,429–16,454, doi:10.1029/91JB00899.

Vinnik, L.P., Kosarev, G.L., and Makeyeva, L.I., 1984, Anisotropy of the lithosphere from the observations of *SKS* and *SKKS*: Proceedings of the U.S.S.R. Academy of Sciences: Atmospheric and Oceanic Physics, v. 278, p. 1335–1339.

Vinnik, L.P., Farra, V., and Romanowicz, B., 1989, Azimuthal anisotropy in the Earth from observations of *SKS* at Geoscope and NARS broadband stations: Bulletin of the Seismological Society of America, v. 79, p. 1542–1558.

West, J.D., Fouch, M.J., Roth, J.B., and Elkin-Tanton, L.T., 2009, Vertical mantle flow associated with a lithospheric drip beneath the Great Basin: Nature Geoscience, v. 2, p. 439–444, doi:10.1038/ngeo526.

Yuan, H., and Romanowicz, B., 2010, Lithospheric layering in the North American craton: Nature, v. 466, p. 1063–1068, doi:10.1038/nature09332.

Yuan, H., Romanowicz, B., Fischer, K.M., and Abt, D., 2011, 3-D shear wave radially and azimuthally anisotropic velocity model of the North American upper mantle: Geophysical Journal International, v. 184, p. 1237–1260, doi:10.1111/j.1365-246X.2010.04901.x.

Zheng, L., Gordon, R.G., and Kreemer, C., 2014, Absolute plate velocities from seismic anisotropy: Importance of correlated errors: Journal of Geophysical Research, v. 119, p. 7336–7352, doi:10.1002/2013JB010902.

Manuscript received 14 January 2015
Revised manuscript received 28 April 2015
Manuscript accepted 25 May 2015

Printed in USA